Supplementary Material

Engineering of hierarchical S-scheme 2D/3D heterojunction with graphdiyne (g-C_nH_{2n-2}) coated 3D porous $CoAl_2O_4$ nanoflower for highly efficient photocatalytic H_2 evolution

Xuqiang Hao[1]*, Wei Deng[1], Yu Fan and Zhiliang Jin*

School of Chemistry and Chemical Engineering, Ningxia Key Laboratory of Solar Chemical Conversion Technology, Key Laboratory for Chemical Engineering and Technology, State Ethnic Affairs Commission, North Minzu University, Yinchuan 750021, P.R.China

E-*mail address*: haoxuqiang@126.com (X. Q. Hao), zl-jin@nun.edu.cn (Z. L. Jin)

Experimental

1. Reagents

All of the chemical reagents were analytical grade and used without further purification. Cobalt nitrate hexahydrate ($Co(NO_3)_2 \cdot 6H_2O$), Aluminum nitrate nonahydrate ($Al(NO_3)_3 \cdot 9H_2O$), urea(CH_4N_2O) and ammonium fluoride (NH_4F) were purchased from Aladdin Reagent Co., Ltd. Absolute ethanol were purchased from Tianjin Damao Chemical Reagent Co, Ltd. Deionized water was utilized throughout the experiments.

2. Synthesis of photocatalysts

2.1 Synthesis of 3D nanofloral CoAl-LDHs

A urea hydrolysis reaction was used to synthesize CoAl-LDHs without surfactant. 0.80 mmol $Co(NO_3)_2 \cdot 6H_2O$, 0.40 mmol $Al(NO_3)_3 \cdot 9H_2O$, 4 mmol NH_4F and 28 mmol urea were mixed in 40 mL DI water and the mixed solution was continuously stirred for 1 h. The solution was transferred into a 100 mL Teflon-lined stainless steels autoclave. The autoclave was sealed and heated at 90 °C for 8 h in an electric blower drying box. After cooling to room temperature, the obtained pink CoAl-LDHs were thoroughly cleaned with DI water and ethanol. The prepared powder was dried in air at

60 °C for 12 h and named as CoAl-LDHs.

2.2 Synthesis of 3D porous CoAl$_2$O$_4$ nanoflowers

The collected CoAl-LDHs precursor powders were put in a porcelain boat and calcinated at 750 °C for 2 h with a heating rate of 5 °C min^{-1}. Afterwards, porous 3D flower-like CoAl$_2$O$_4$ microspheres were obtained. The catalysts calcined at 750 °C were named CoAl$_2$O$_4$. The catalysts calcined at 650 °C, 750 and 850 °C were named CoAl$_2$O$_4$-650, CoAl$_2$O$_4$-750 and CoAl$_2$O$_4$-850 catalysts, respectively.

2.3 Synthesis of Graphdiyne nanosheets

Graphdiyne (GDY) nanosheets was prepared according to the cross-coupling reaction of hexaethynylbenzene. Briefly, 35 mL tetrahydrofuran (THF) was added to a three-necked round-bottomed flask (250 mL), whereafter 4.30 mL trimethylsilylacetylene was added, then dropwise injected 12 mL n-butyllithium (2 M in THF) to the above system and maintained 78 °C for 0.5 h under continuous magnetic stirring. Continuing to add 20 mL zinc chloride anhydrous (2 M in 2-Methyl-THF), after stirring for 0.5 h, heat up to the ambient temperature. It should be noted that the above process proceeds in a nitrogen atmosphere. 1.10 g hexabromobenzene, 0.50 g Pd (PPh$_3$)$_4$ and 25 mL toluene (Extra Dry) were added to the above solution keeping stirring at 80 °C for 72 h protected by N$_2$. The obtained products were acidized by 20 mL HCl (1 M) extracted with ethyl acetate and washed with saturated salt solution and pure water. It was then dried with Na$_2$SO$_4$ (anhydrous), and the residue was purified by column chromatography (silica gel, n-hexane: dichloromethane = 17:3), about 20% yield of hexakis [(trimethylsilyl)ethynyl] benzene was acquired. The pale yellow solid was dissolved in 20 mL of tetrahydrofuran (THF), and 2 mL of tetrabutylammonium fluoride (1 M in THF) was added. The mixture was stirred at 8°C for 10 minutes. The solution was diluted by ethyl acetate, washed with saturated salt solution three times, and dried with anhydrous Na$_2$SO$_4$. Finally, the products were dissolved in 25 mL pyridine (99.5%, Extra Dry), then slowly dropped over 24 h in the solution containing 50 mL pyridine and 0.50 g CuI at 60 °C. The reaction was kept at 60 °C for 48 h. The final product was washed with ultrapure water and ethanol several times. Subsequently, the solution was washed with ammonium hydroxide to remove copper ions in the system and dried at 60 °C overnight. The as-prepared sample was noted as graphdiyne.

Fig. S1. The fabrication process of GDY.

2.4 Synthesis of GDY/CoAl$_2$O$_4$ composites

To begin with, 0.06 g CoAl$_2$O$_4$ was weighed and mixed with different masses of GDY (0.006 g, 0.009 g, 0.012 g, 0.15 g, 0.018 g) in a beaker, then 10 mL of anhydrous ethanol and 5 mL of deionized water were added to form a homogeneous solution by sonication and stirred overnight, and the resulting product was washed with deionized water and ethanol and 60 °C and dried. The resulting product is denoted as GCA-X (X=10, 15, 20, 25 and 30), where "X" represents the loading amount of GDY.

3. Photocatalytic hydrogen evolution

Photocatalytic hydrogen production experiment was performed in a glass bottle with a total volume of 62 mL. Typically, 6 mg of the photocatalyst and 10 mg EY were dispersed in 30 mL 15v/v% triethanolamine (TEOA) aqueous solution. Then use N$_2$ to remove air before irradiation. Then, a 5 W LED lamp in a nine-channel photocatalytic reaction system was employed as the visible-light source. Subsequently, 0.5 mL gas was extracted from the reaction flask every 1 h to analyze by the gas chromatography (Tianmei GC7900, TCD, 13 X columns, N$_2$ as carrier gas).

4. Detailed DFT Calculation

We constructed the heterostructure based on the hexagonal graphdiyne (space group: P6/mmm)

and the cubic $CoAl_2O_4$ (space group: Fd-3m). We first cleaved the $CoAl_2O_4$-(111) surface and then orthogonalized it through a transformation matrix. The graphdiyne-(001) plane was also constructed and then transformed to comply with the 3x1x1 supercell of the $CoAl_2O_4$-(111) slab model. The vertical heterojunction was built with a lattice mismatch less than 3%. We performed structure optimization based on the density functional theory (DFT) implemented in the Vienna Ab initio Simulation Package (VASP) [1]. The projector-augmented wave (PAW) pseudopotentials was adopted to describe the ion cores, and we used the Perdew-Burke-Ernzerhof (PBE) functional of generalized gradient approximation (GGA) to compute the exchange-correlation interactions of valence electrons [2, 3]. A cutoff energy of 400 eV and the Γ-centered 2 x 3 x 1 k-point mesh were employed to integrate the Brillouin zone (BZ). The dispersion interactions were corrected with the D3 method developed by Grimme [4]. The convergence standard for force and energy during the structure relaxation were 0.03 eV/Å and $1x10^{-5}$ eV, respectively.

5. Electrochemical measurements

Electrochemical performance was tested by VersaStat 4-400 conventional three-electrode battery. 0.2 M Na_2SO_4 aqueous solution as electrolyte, saturated glycerin electrode (SCE) as reference electrode and platinum foil as counter electrode. 5 mg photocatalyst was mixed with 200 μL Nafion solution ($C_9H_7BrN_2S$:C_2H_6O = 1:9), then obtained suspension was slowly dropped onto the surface of 1 x 1 cm^2 fluorine-doped tin oxide (FTO) glass surface. The working electrode was obtained after drying under infrared light. The instantaneous photocurrent cure was measured at bias voltage of 0.2 V using 300 W Xe lamp with a 420 nm cutoff filter. Electrochemical impedance spectra (EIS) were measured at applied potential of 0.2 V vs. SCE. The electrocatalytic activity were determined by linear sweep voltammetry (LSV), and cyclic voltammetry (CV) were determined at scan rate of 5 mV s^{-1}. Under dark conditions, Mott-Schottky plots of the catalysts were measured at -1.0 ~ 1.0 V vs. SCE, and the flat band potentials of catalyst was obtained.

6. Characterization

The crystal structure was analyzed by X-ray diffraction (XRD) (Rigaku UItima III x-ray diffractometer) at 40 kV and 30 mA. The molecular structure of the material was analyzed by Fourier transform infrared spectrometer (FT-IR, WQF-520A). The morphology and microstructure

of the catalysts were characterized by field emission scanning electron microscopy (SEM: JSM-6701F, JEOL, 50 kV) and low-resolution transmission electron microscopy (TEM) and high-resolution transmission electron microscope (HRTEM) images were recorded by JEM-2100 electron microscope at 200 kV. The elemental composition, valence state and optical properties of the samples were characterized by X-ray photoelectron spectroscopy (XPS: ESCALAB Xi$^+$). In-situ XPS spectra were obtained from an electron spectrometer (XPS: ESCALAB Xi$^+$) under the UV-light irradiation (λ=310 nm). Zeta potential of catalyst was recorded with Litesizer 500 in pure water. The UV-vis diffuse reflectance spectra (Benchmark calibration using $BaSO_4$ powder) and UV-vis absorption spectra of all catalysts were characterized by PerkinElmer Lambda-750 UV-vis-NIR spectrometer. The fluorescence (PL) spectra and time-resolved fluorescence emission spectra of the samples were obtained by FLUORO-MAX-4 spectrophotometer and Horiba Jobin Yvon Data Station HUB, respectively.
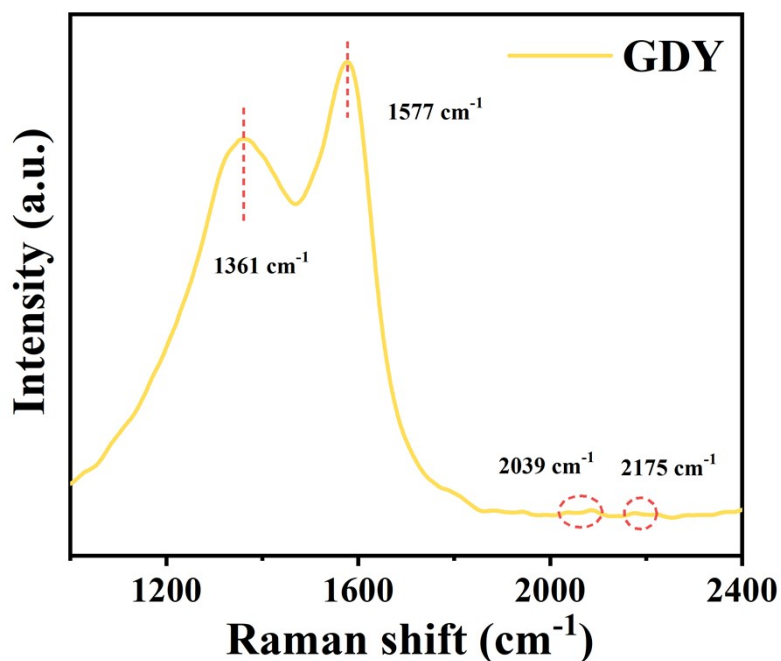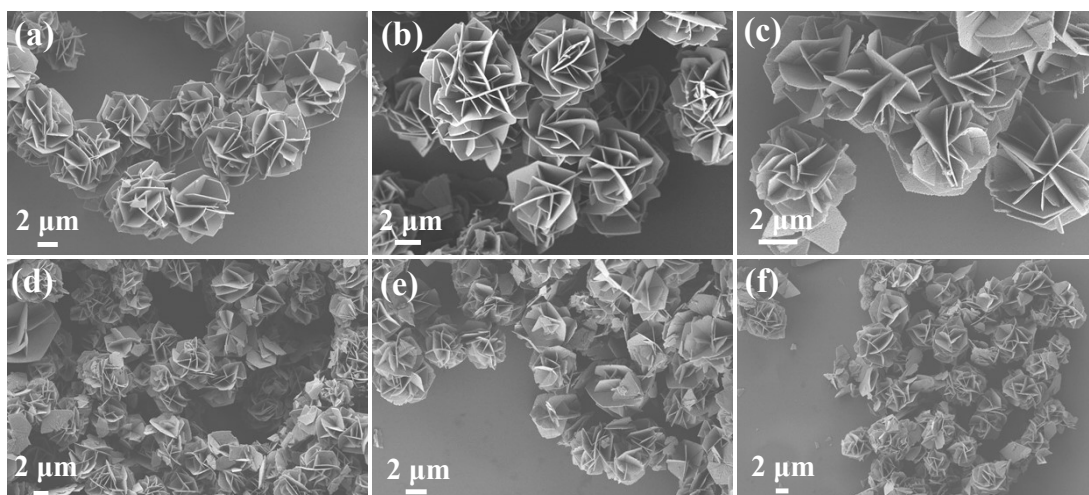

Fig. S2. Raman patterns of GDY.

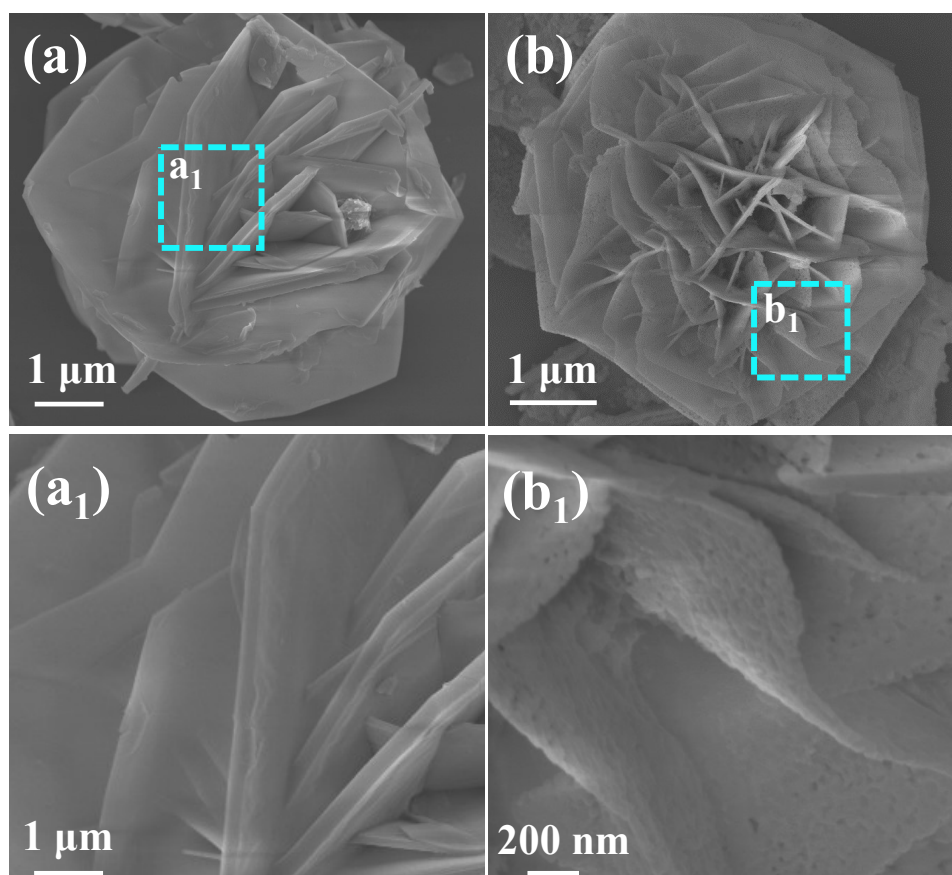**Fig. S3.** SEM images of (a-d) $CoAl_2O_4$ and (e, f) GCA.

Fig. S4. The SEM images of (a, a₁) CoAl-LDHs; (b, b₁) $CoAl_2O_4$.
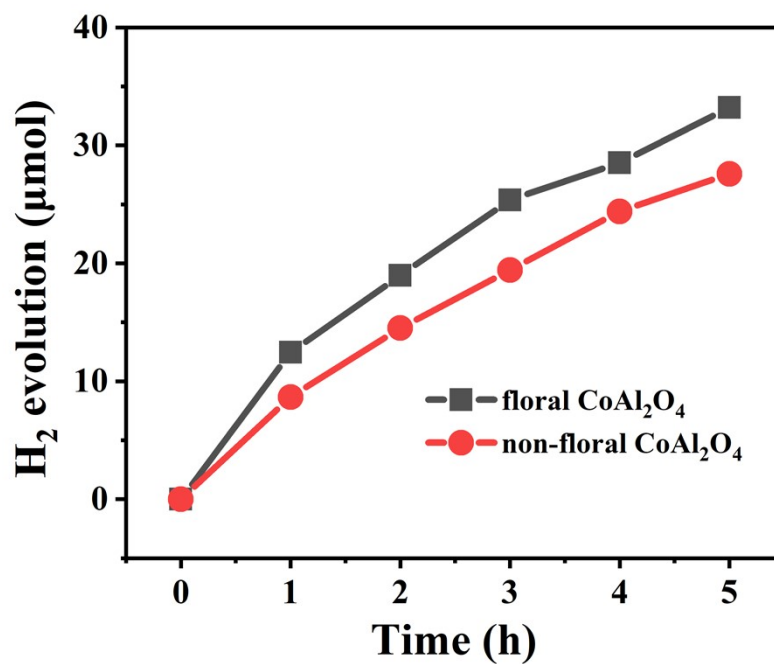
Fig. S5 Photocatalytic hydrogen evolution activities of floral $CoAl_2O_4$ and non-floral $CoAl_2O_4$.
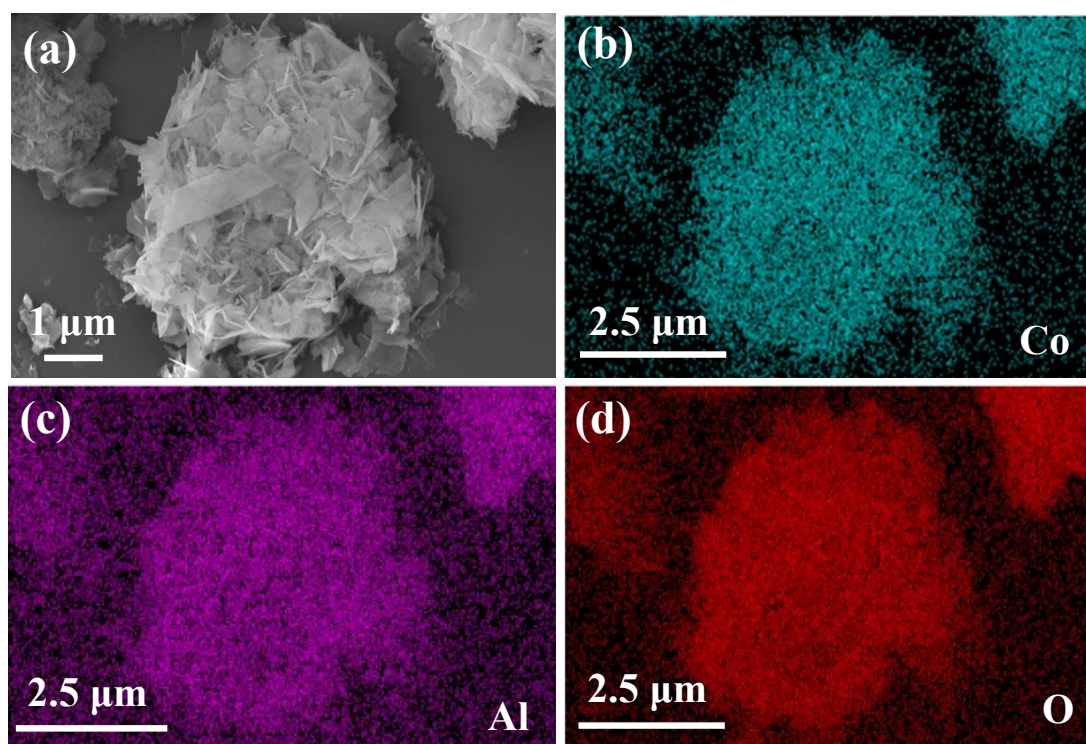

Fig. S6. Elemental mappings (b-d) of the area in (a) for non-floral $CoAl_2O_4$.

Table S1. Comparison of GDY-based composites for photocatalytic H_2 production.

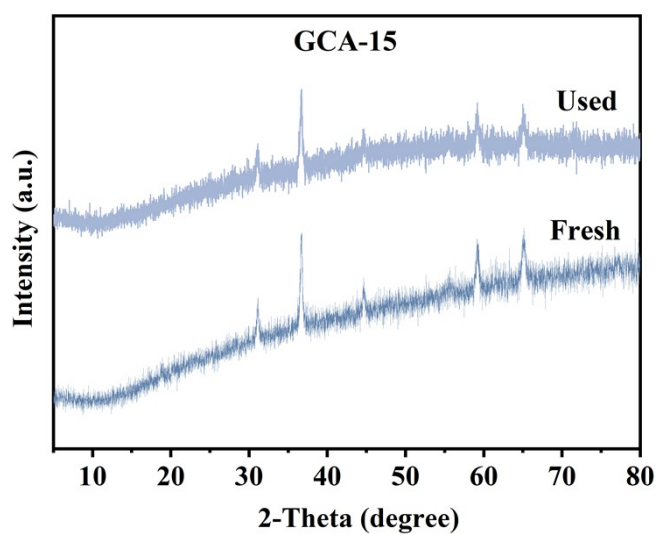| Photocatalysts	Light sources	Sacrificial reagent	Activity (μmol h^{-1} g^{-1})	Ref.
GDY/CoAl$_2$O$_4$	$\lambda \geq 420$	TEOA	5009.28	**This work**
CoMoO$_4$/GDY	$\lambda \geq 420$	TEOA	2420.00	[5]
Co-Co PBA/GDY	$\lambda > 420$	TEOA	1938.60	[6]
NiCo$_2$O$_4$/GDY	$\lambda > 420$	TEOA	4840.00	[7]
Co$_9$S$_8$-GDY-CuI/GDY	$\lambda > 420$	TEOA	1411.82	[8]
GDY@C$_3$N$_4$-3/Pt	$\lambda > 420$	TEOA	798.00	[9]

Fig. S7. XRD patterns of hydrogen production fresh GCA-15 and used GCA-15 comparison chart.
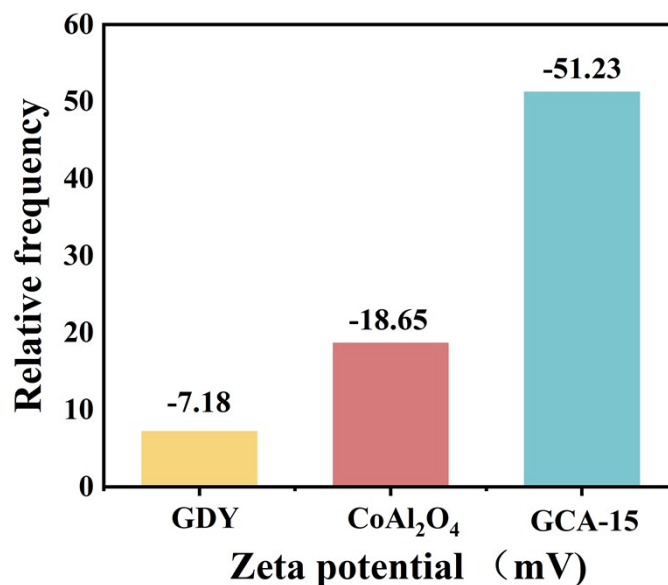
Fig. S8. The Zeta potential of GDY, CoAl$_2$O$_4$ and GCA-15.

References

[1] G. Kresse, J. Furthmüller, Efficient iterative schemes for ab initio total-energy calculations using a plane-wave basis set, Phys. Rev. B 54 (1996) 11169-11186.

[2] H. Levämäki, M. Kuisma, K. Kokko, Projector Augmented-Wave Method. Physical Review B 50 (1994) 17953-17979.

[3] Perdew, Burke, Ernzerhof, Generalized gradient approximation made simple. Phys. Rev. Lett. 18 (1996) 3865-3868.

[4] S. Grimme, J. Antony, S. Ehrlich, H. Krieg, A consistent and accurate ab initio parametrization of density functional dispersion correction (DFT-D) for the 94 elements H-Pu. J. Chem. Phys. 132 (2010), 154104.

[5] L. Fan, Y. Wang, X. Guo, Z. Jin, Type-II CoMoO$_4$/Graphdiyne heterojunction promotes visible-light-driven photocatalytic hydrogen production activity, Sep. Purif. Technol. 332 (2024) 125786.

[6] K. Wang, M. Wang, H. Xie, S. Li, X. Kong, Z. Jin, Rational construction of graphdiyne (g-C$_n$H$_{2n-2}$) coupling with Co-Co PBA S-scheme heterojunctions for efficient photocatalytic hydrogen production, Sep. Purif. Technol. olume 322 (2023) 124286.

[7] K. Wang, M. Wang, H. Xie, S. Li, X. Kong, Z. Jin, Rational construction of graphdiyne (g-

CnH2n−2) coupling with Co-Co PBA S-scheme heterojunctions for efficient photocatalytic hydrogen production, Sep. Purif. Technol. olume 322 (2023) 124286.

[8] Z. Jin, H. Li, J. Li, Efficient photocatalytic hydrogen evolution over graphdiyne boosted with a cobalt sulfide formed S-scheme heterojunction, Chin. J. Catal. 43 (2022) 303-315.

[9] C. Wang, X. Han, Q. Xu, Y. Sun, J. Arbiol, M. Ghazzal, J. Li, In situ construction of graphdiyne based heterojunctions by a deprotection-free approach for photocatalytic hydrogen generation, J. Mater. Chem. A 11 (2023) 3380-3387.